Computers & Geosciences 36 (2010) 489–499

Contents lists available at ScienceDirect

Computers & Geosciences

journal homepage: www.elsevier.com/locate/cageo

Dual-scale validation of a medium-resolution coastal DEM with terrestrial LiDAR DSM and GPS

Seamus Coveney *, A. Stewart Fotheringham, Martin Charlton, Timothy McCarthy

National Centre for Geocomputation, National University of Ireland, Maynooth, County Kildare, Ireland

ARTICLE INFO

Article history:
Received 5 February 2009
Received in revised form
26 September 2009
Accepted 8 October 2009

Keywords:
DEM error
Terrestrial LiDAR DSM
GPS
Coastal flooding

ABSTRACT

The use of medium-resolution photogrammetric-derived Digital Elevation Models (DEMs) to model coastal inundation risk is commonplace in the geosciences. However, these datasets are often characterised by relatively large and loosely defined elevation errors, which can seriously limit their reliability. Post-processed and static RTK dual-frequency GPS data and very high-resolution Terrestrial Laser Scanning DSM data are used here to quantify the magnitude and spatial distribution of elevation error on a 10 km coastal section of a medium-resolution photogrammetric DEM. The validation data are captured at two scales and spatial-resolutions to minimise the risk of spatial bias in the validation results. The strengths and shortcomings of each validation dataset are assessed, and the complimentary value of GPS and Terrestrial Laser Scanning for external validation is demonstrated. Elevation errors highlighted in the photogrammetric DEM are found to be significantly larger than suggested by the data suppliers, with a tendency for the larger errors to occur with increasing proximity to the coastline. The results confirm the unsuitability of the DEM tested for the local spatial modelling of coastal inundation risk, highlighting difficulties that may be prone to occur when similar DEM datasets are used in coastal studies elsewhere.

1. Introduction

Digital Elevation Models (DEMs) are routinely used for the spatial modelling of coastal flood risk (Gornitz et al. 2002; Leatherman et al. 2003; Webster (2005)) for sea-level rise assessment (Cowell and Zeng, 2003; Dobosiewicz 2001) and for modelling river flood sensitivity (Brasington et al. 2000; Cobby et al., 2001; Gomes Pereira and Wicherson, 1999). The accuracy of the elevation component of medium-resolution (30–100 m) DEMs may arguably be sufficient for broad-scale regional or national assessments but the errors that typically occur within these DEMs tend to make them less suitable for modelling processes at sub-regional and local scales (Bryan et al. 2001; Gornitz et al. 2002; McInnes et al. 2003). It is important to note that even relatively modest elevation errors can lead to substantial spatial misclassification of inundation risk on flood-prone coastlines due to the multiplication of elevation error by the gradient factor that characterises flood-prone coastal areas (Douglas et al. 2001; Pugh 2004). Large errors will generally make a DEM unsuitable for spatial prediction of coastal inundation risk.

The increasing availability of high-accuracy Aerial Laser Scanning (ALS) data means that the use of medium-resolution DEMs for flood prediction is likely to decrease in the future. However, ALS data are expensive to capture and process, and are often not available at all, so in many cases DEM users are limited to the use of regional-coverage, medium-resolution (30–100 m) DEM data. Elevation errors in these DEMs typically lie within the range of ± 3 to ± 5 m (Lane et al. 2003; Lee et al. 2005; Oksanen and Sarjakoski 2005). The use of a single error statistic to describe DEM error is problematic, because it provides no information about the spatial distribution of elevation error. This makes it difficult to establish whether error at the coast is likely to be smaller or larger than quoted error. The limitations of medium-resolution DEM data for the prediction of coastal inundation risk are well known (Bryan et al. 2001; Dobosiewicz 2001; Gornitz et al. 2002; McInnes et al. 2003). However, studies that apply DEM data to the delineation of flood risk are often less concerned with the detailed assessment or quantification of DEM error. Furthermore, the studies that do focus on the quantification of DEM error are often less concerned on the application of the data than the refinement of quantification methods. The literature on the subject of DEM error quantification includes mathematical modelling (Heuvelink 1998; Ehlschlaeger 2002; Oksanen and Sarjakoski 2005; Wechsler and Kroll 2006) with limited ground sampling (Fisher 1998, Van Niel et al., 2004; Van Niel and

* Corresponding author. Tel.: +353 1 7086180; fax: +353 1 7086456.
E-mail addresses: seamus.coveney@nuim.ie (S. Coveney), stewart.fotheringham@nuim.ie (A. Stewart Fotheringham), martin.charlton@nuim.ie (M. Charlton), tim.mccarthy@nuim.ie (T. McCarthy).

0098-3004/$ - see front matter © 2010 Published by Elsevier Ltd.
doi:10.1016/j.cageo.2009.10.003

Austin 2007) and validation by direct measurement (Huising and Gomes Pereira, 1998; Lane et al., 2003; Lee et al., 2005; Oksanen and Sarjakoski, 2005). External validation can provide detailed measurements of absolute elevation error, but validation accuracy is strongly reliant on the accuracy of the validation data used.

Studies that use external validation to quantify DEM elevation error demonstrate the range of validation data that can be used, and the variety of medium-resolution DEMs that can be tested. Chang et al. (2004) and Lee et al. (2005) use Real Time Kinematic (RTK) GPS data to validate DEMs derived from spaceborne Synthetic Aperture RADAR (SAR) and photogrammetry. Baldi et al. (2002) use RTK-GPS to validate high-resolution photogrammetric-DEMs. Webster (2005) uses RTK-GPS to validate ALS-derived Digital Surface Model (DSM) data, and Oksanen and Sarjakoski (2005) use ALS as an external validation dataset for the definition of elevation error in a medium-resolution DEM.

Minimum relative accuracies for validation data and DEM data are stipulated within a number of different guidelines documents (ANSI-INCITS, 1998; FGDC, 1988; Flood 2004; Höhle and Potuckova, 2006).

This paper aims to clearly quantify elevation error in a medium-resolution coastal DEM in a manner that demonstrates the shortcomings of this type of data for the spatial modelling of coastal inundation risk. The primary aims of this paper are:

to quantify the magnitude and spatial distribution of elevation error in a 10 km sample section of a coastal photogrammetric DEM using verifiably-accurate GPS and TLS external validation data captured at two spatial-resolutions and scales,
to determine the suitability of this DEM for the spatial modelling of coastal flood risk in the area studied, and to highlight issues that may occur when similar DEM data are considered for use in flood modelling studies elsewhere.

The limitations of TLS in areas where extremely dense ground vegetation is dominant are also highlighted, and this problem is rectified before the TLS data are used to externally validate the medium-resolution DEM. The generic problem of laser penetration to ground level (from any laser scanning platform) in areas where extremely dense ground vegetation cover predominates is also briefly discussed in the context of the need for future work.

2. Methods

2.1. Selection of validation datasets

Two alternate validation datasets are used to provide comparative assessments of DEM error at different spatial-resolutions and scales. High-accuracy post-processed GPS (captured at a mean sampling resolution of 65×65 m^2), and static-capture RTK-GPS (captured at a mean sampling resolution of 18×18 m^2) are combined to generate a set of 670 GPS validation points (at a mean sampling resolution of 40 m). A very high-resolution (1×1 m^2) TLS DSM dataset is also generated (overlapping the GPS validation survey area) to validate a section of the DEM tested. Dual-frequency post-processed and RTK-GPS data are used for validation because of their very high absolute accuracy (Section 2.4) and their capacity to penetrate ground vegetation in the chosen study area.

The potential of single laser returns TLS for the enhancement of ALS surveys has received some attention in the geosciences literature (Iavaronea and Vagners, 2003; Ruiz et al., 2004) and its potential as a standalone tool in coastal management has received some attention also (USGS, 2006) but it has not (as far as we are aware) yet been used for DEM validation. A TLS DSM *x,y,z* point dataset is used in this study because of its high acquisition accuracy and extremely high-resolution (the raw TLS data consisted of 27 million points at a mean sampling resolution of 6 cm) and because of the absence of ALS data for the study area (and the majority of the Irish coastline). A range of issues had to be overcome before these data could be used for validation purposes. Many TLS scanners are not capable of segregating first and last laser returns, so the problem of residual ground vegetation error (which can sometimes be removed when first and last returns are available) had to be overcome by other means before the TLS data could be used to validate medium-resolution DEM error.

2.2. Study area selection

Elevation errors in the medium-resolution DEM tested here are quoted at approximately ± 3 m by the data suppliers. This suggests that the data may be unsuitable for the spatial modelling of coastal inundation risk. However, the recognised relationship between topographical complexity and DEM elevation error (Bolstad and Stowe, 1994; Fisher, 1998; Fisher and Tate, 2006; Holmes et al., 2000) does imply that elevation errors in the relatively flat shallow-gradient study area might perhaps be smaller than elsewhere. If this were the case, it might provide some justification for the use of medium-resolution DEMs in the spatial prediction of flood risk in similar topographical contexts elsewhere.

This study focuses on the measurement of elevation error in a medium-resolution (10 m) DEM on a 10 km test-section of shallow-gradient coastline in the Shannon estuary in Ireland (Fig. 1). The DEM tested was supplied at a spatial-resolution of 10×10 m^2, but (typically of DEMs derived from photogrammetry) is derived from interpolation of a much lower-resolution set of ground control and photogrammetric-derived points (see Section 4). The study area was selected on the basis of inundation impact vulnerability. The southwest coast of Ireland is subject to a combination of regional isostatic submergence (Devoy, 2008) global climate-induced sea-level rise (IPCC, 2007) and north Atlantic storm surges (Orford, 1989). The area also supports estuarine saltmarsh habitat (Fig. 1) which is protected under the EU habitats Directive (EU 1992). This habitat is particularly prone to erosion and landward retreat when coastal inundation risk increases (Hughes and Paramor, 2004; Wolters et al., 2005).

2.3. Validation data capture

External-validation data were captured in the study area in the form of post-processed dual-frequency GPS data (at a mean ground sampling resolution of 65×65 m^2), RTK-GPS (at a mean sampling resolution of 18×18 m^2), and error-adjusted TLS survey data (captured at a mean spatial-resolution of 6 cm and processed to a mean spatial-resolution of 1×1 m^2 *x,y,z* points). The post-processed dual-frequency GPS data were captured across an area of 100 ha along a 10 km section of coastline (at a time when the Irish RTK correction system was available in beta mode only). The static RTK-GPS survey data (captured when the RTK correction system was fully implemented by the Irish national mapping agency) covered 11 ha, along approximately 1.25 km of coastline. The TLS data were captured across 9 ha along 1 km of coastline. The post-processed GPS survey (Fig. 2a). static RTK-GPS (Fig. 2b) and TLS survey (Fig. 2c) all overlapped spatially.

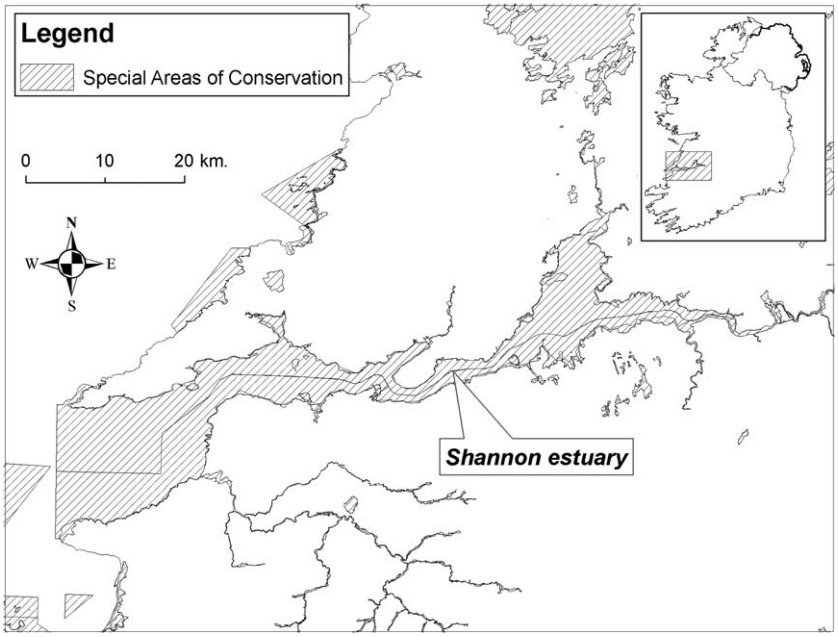

Fig. 1. Location of, and SAC designations within Shannon estuary (Source: National Parks and Wildlife Service).

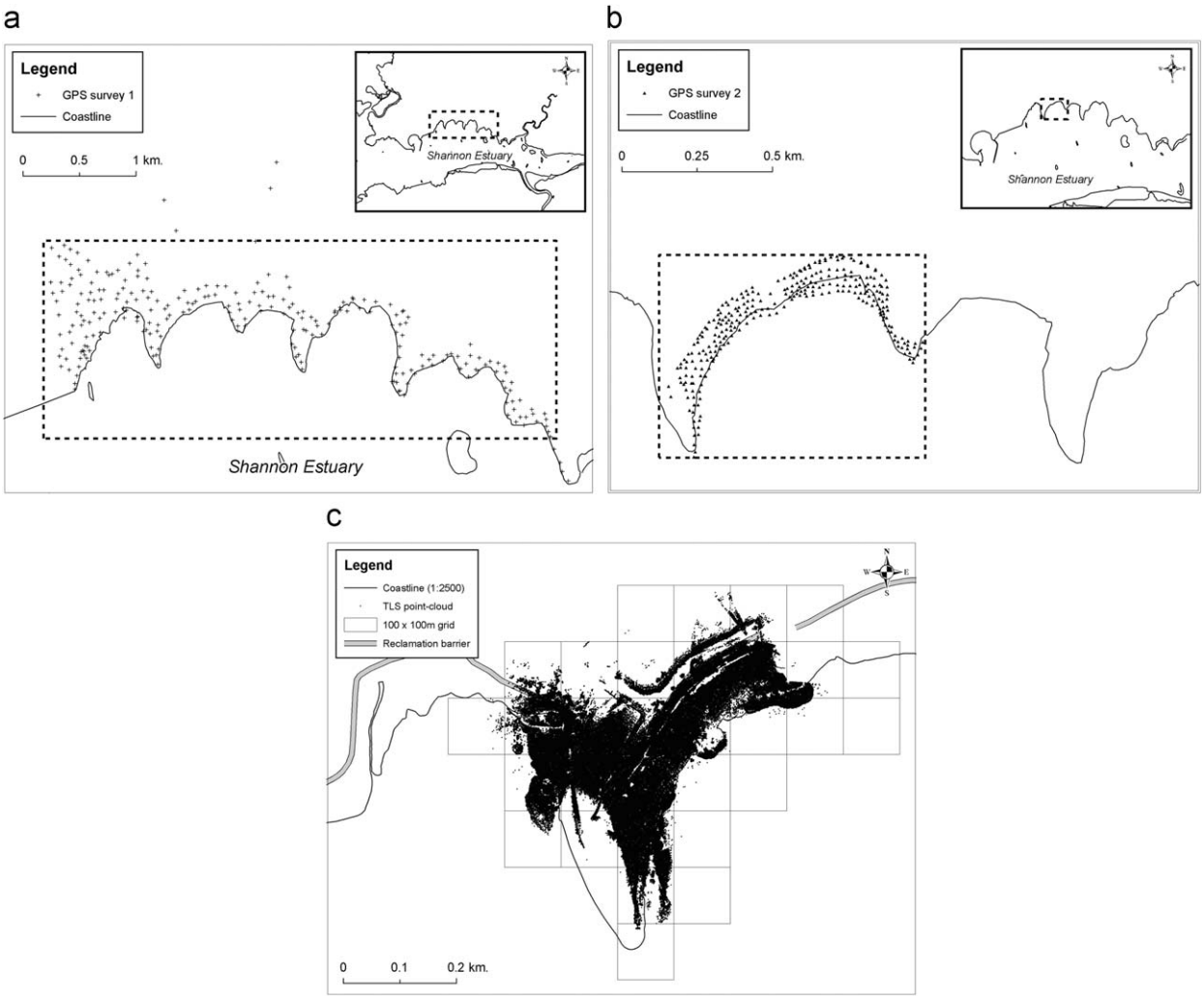

Fig. 2. . (a): Post-processed GPS points captured in study area. (b): (a) Static RTK-GPS points captured in study area.

2.4. Accuracy of the validation data

It is important that the relative accuracies of validation data and DEM data meet minimum requirements (ASPRS, 1989). Elevation accuracies that can be achieved with post-processed and RTK-GPS range from ± 0.01 at best to ± 0.1 m at worst (Gao and Chen, 2004). The acquisition accuracy of laser scanning is generally accepted to be in the range of ± 0.05–0.25 m (Hodgson and Bresnahan 2004; Huising and Gomes Pereira 1998). However, the accuracy of GPS data does depend on the data capture methods used. Elevation errors within laser scan data captured in densely vegetated areas can be quite large, with errors of up to 1 m being noted in a number of studies (Cobby et al., 2001; Lohani and Mason, 2001; Palamara et al., 2007; Sithole and Vosselman, 2004). Very high acquisition accuracies were achieved in the GPS and TLS surveys captured in the study area (Section 3). However, ground vegetation error of approximately 1 m did occur in the TLS data, so this had to be dealt with before the data could be used for validation purposes. The static RTK-GPS data (which were themselves characterised by errors of ± 0.03 m) were used to quantify and remove TLS vegetation error prior to its use for the external validation of the medium-resolution DEM in the study area.

2.5. Optimised interpolation of the medium-resolution DEM

The medium-resolution DEM data used in this study were purchased from the national mapping agency in *x,y,z* point form (rather than in raster format) to avoid the potential for undefined interpolation errors to complicate the quantification of absolute DEM error. The *x,y,z* point data were then interpolated in a controlled manner in order to minimise the introduction of interpolation error prior to external validation. Optimisation of the interpolation of the data involved universal kriging elevation trend segregation, semi-variogram selection and interpolation Cross Validation.

2.6. External validation

A 10 km section of the photogrammetric DEM was subsequently externally validated using the GPS data (combined into a single validation set at a mean ground sampling resolution of 40×40 m^2), and the spatially-coincident (though more geographically confined) TLS DSM point data. External validation was carried out using ArcGIS/ArcInfo Geostatistical Analyst, utilising the GPS and TLS data in turn as a test dataset to validate the optimised interpolation of the photogrammetric DEM.

3. Analysis

3.1. Data capture

3.1.1. Post-processed dual-frequency GPS

Two-hundred and forty GPS points were captured using a Trimble R8 dual-frequency GPS receiver using FastStatic point capture (on 8 min residence times) and these points were post-processed against RINEX correction data from the closest (18 km) GPS correction station (Fig. 2a). The mean spatial resolution of these points was 65 m. Post-processing (conducted using Trimble Geomatics Office software) highlighted elevation errors of less than 0.03 m within 95% of these post-processed GPS validation points (Table 1).

3.1.2. Static RTK-GPS

The limitations on ground sampling resolution that were imposed by the requirement for long residence times in the FastStatic GPS survey were overcome to a large extent within the static RTK-GPS survey. Four-hundred and thirty static survey points were captured in two adjacent survey sections (Fig. 2b) using a Trimble R8 GPS receiver operating in static RTK mode. The static RTK-GPS survey area covered approximately 10 ha along approximately 1.25 km of coastline at a mean spatial resolution of 18 m. Ninety-five percent of the internal GPS elevation errors highlighted during RTK correction of the 430 RTK-GPS *x,y,z* data points were in the range of 0.03 m (Table 1) confirming their suitability as an external validation dataset.

3.1.3. High-resolution TLS survey

Eleven overlapping TLS scans were required in order to cover the entire TLS survey area (Fig. 3) so it was necessary to ensure that scan co-registration was conducted accurately. The TLS scans were linked by 20 RTK-GPS controlled HDS (High Definition Surveying) targets (Fig. 3). Scanning was conducted using a Leica ScanStation TLS scanner using Leica Cyclone (v5.8) surveying software. This scanner operates in single-return laser pulse mode and is capable of capturing survey points at an accuracy level of ± 0.003 m within a data capture range of 100 m (Leica Geosystems, 2007). The accuracy with which the TLS data were acquired was ultimately verified by external validation with GPS during the processing of the TLS data in GIS (see Section 3.2) to

Table 1
Elevation errors detected in the entire set of 670 GPS points.

Vertical	Accuracy
Count	670
Min.	± 0.002
Max.	± 0.099
Mean	± 0.015982
Std. Dev.	0.008905
Error range	± 1cm–25% ± 1.5cm–53% ± 2cm–75% ± 3cm–95%

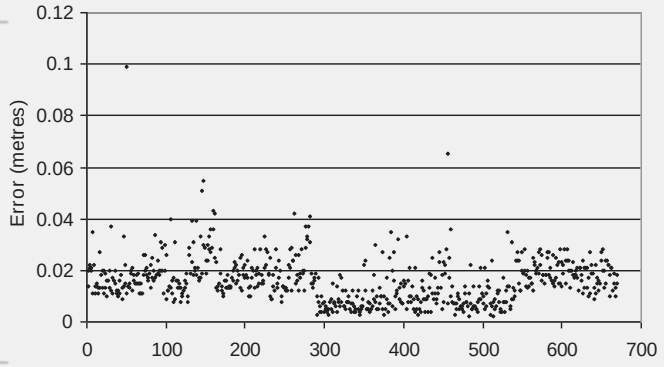

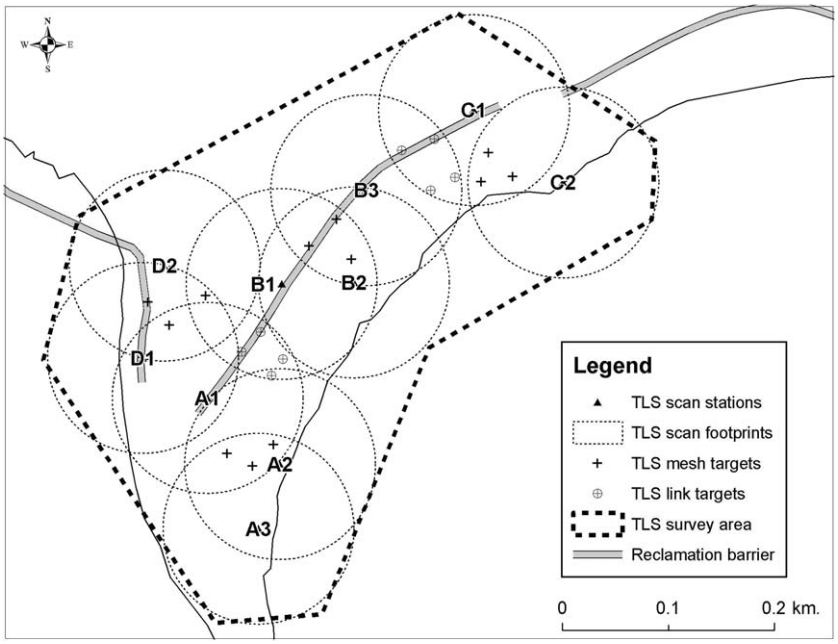

Fig. 3. (a) Minimum areal footprints (A1–D2) of scans surveyed in field, (b) mesh target clusters (at_1_2 through to dt_3_4) used to co-register scan groups, and (c) link targets (abl_1 through to bcl_4) used to mosaic adjacent scan groups.

Table 2
The largest horizontal and vertical errors introduced in each successive step of the co-registration process (*maximum horizontal and vertical errors for each co-registration step are highlighted in bold*).

Scans integrated	reg_phase	target_ID	horz_err.	vert_err.
B1 & B2	1	abl_2	± 0.026	± 0.007
C1_C2 & B1_B2_B3	2	bcl_2	± 0.006	± 0.011
A2_A3_A1a & A1b_D1_D2	2	abl_4	± 0.045	± 0.008
Shan_lidar_reg_101 & Shan_lidar_reg_102	3	abl_3	± 0.017	± 0.014
Shan_lidar_reg_101 & Shan_lidar_reg_102	3	abl_1	± 0.043	± 0.005

ensure that it would not adversely affect the identification of medium-resolution DEM error.

3.2. TLS data quality

3.2.1. Accuracy of TLS co-registration

The Leica scanner/software system is capable of semi-automatic target recognition and co-registration with minimal user input. Clusters of three HDS targets were set up in order to co-register groups of adjacent scans into three-scan sets. These were in turn co-registered with each of their adjacent scan sets using three additional HDS targets (Fig. 3). Small errors were introduced during co-registration due to imperfect target matching. The largest horizontal error introduced during co-registration (determined using the Leica software) was 0.045 m and the largest elevation error introduced was 0.014 m (Table 2).

3.2.2. Accuracy of TLS georeferencing

TLS georeferencing was carried out using the defined GPS-positions of the HDS target centres. The co-registered TLS mosaic (containing over 27 million points) was georeferenced to realign it from survey coordinates to Irish National Grid (ING) *x,y* Cartesian map coordinates in Leica Cyclone. Orthometric heights were defined relative to the OSGMO2 (Republic of Ireland) geoid. The largest error detected among the GPS georeferencing coordinates was 0.003 m (Table 3) confirming their suitability for georeferencing the co-registered TLS mosaic. Georeferencing was carried out using affine transformation in Leica Cyclone. The lowest georeferencing errors were achieved using a 4-point (HDS target positions) transformation. Some additional elevation

Table 3
The five largest horizontal and elevation coordinate errors from the seventeen potential georectification targets positions as defined by GPS.

Name	Northing	Easting	Elevation	Horz_err.	Vert_err.
bcl_1	161,167.99	140,066.48	4.75	± 0.014	± 0.002
Bt_1	161,077.02	139,981.41	4.46	± 0.023	± 0.003
Bt_2	161,108.87	140,003.57	4.66	± 0.014	± 0.002
Ct_2_3	161,166.39	140,144.24	2.86	± 0.012	± 0.002
Dt_2	161,002.14	139,885.69	2.29	± 0.010	± 0.002

Table 4
Horizontal and vertical error margins introduced at the RTK-GPS coordinates used to georeference the final T-LIDAR mosaic.

Georectification point	Horizontal error	Vertical error
ct_4	± 0.038	± 0.004
bcl_4	± 0.034	± 0.018
abl_4	± 0.034	± 0.033
dt_2	± 0.03	± 0.047

errors were introduced at this stage (Table 4), the largest being an elevation error of 0.047 m.

3.2.3. Suitability of TLS as validation data

The georeferenced TLS data coverage consisted of approximately 27 million *x,y,z* points at a mean spatial resolution of 0.06 m covering an area of approximately 9 ha (Fig. 2c). The sum of the maximum scanner acquisition error (0.006 m), maximum scan co-registration elevation error (0.014 m) the maximum georeferencing elevation error (0.047 m) and the maximum elevation error in the GPS points used to georeference the TLS scan mosaic (0.003 m) was 0.07 m. Therefore, the acquisition accuracy of the TLS data were approximately half of that which was achieved with GPS. However, very substantial elevation errors persisted in the data due to the presence of very dense ground vegetation, and additional processing was required to remove this error before the TLS data could be used for DEM validation.

The complicating influence of dense ground vegetation in laser scan data is well known (Cobby et al., 2001; Lohani and Mason 2001; Sithole and Vosselman, 2004; Palamara et al., 2007) and the issue can often be rectified by separating first and last laser returns (Hall et al., 2005; Lim et al., 2003; Popescu et al. 2002). However, the best results are generally achieved in forested, wooded or sparse scrubland areas (Hodgson et al., 2003; Hall et al., 2005) where laser penetration to the ground surface is straightforward. However, this can be exceptionally difficult to achieve in coastal saltmarsh areas (Rosso et al., 2006), densely grassed river floodplain areas (Cobby et al., 2001) and dense scrubland areas (Palamara et al., 2007) where ground vegetation errors of up to 1 m can persist after DSM generation. The elevation errors that could be attributed to the presence of dense ground vegetation in TLS data captured for this study were up to 1 m in magnitude. A range of filters were applied to the TLS data to generate a TLS DSM prior to using it to quantify the magnitude of elevation error in the medium-resolution DEM.

3.2.4. Generation of TLS DSM

A Grid-Based, lowest Elevation point Filter (GBEF) was run on the 27 million TLS points in MySQL to identify the lowest

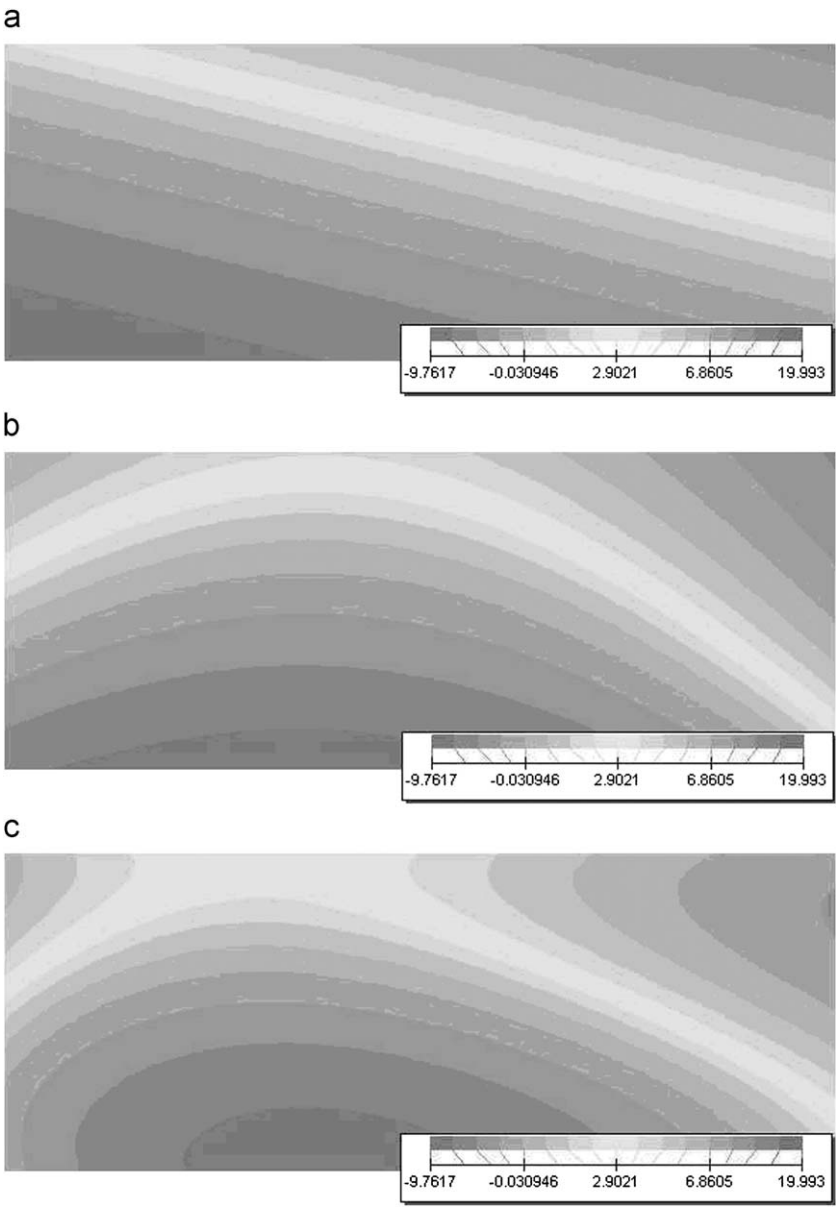

Fig. 4. . (A) first order trend in photogrammetric DEM. (B) Combined first & second order trend. (C) Combined first/second/third order trend.

elevation point in each of a total number of 86,000 1×1 m^2 grid cells across the study area. The resulting set of 86,000 1×1 m^2 *x,y,z* TLS points was further filtered using simple elevation thresholding, polygon masks and local reclassification filters. The threshold elevation value was defined at 0.5 m above the highest point within the flood-prone section of the study area. The polygon mask filter consisted of a simple mask-defined selection of points that lay beyond the boundary of the flood-prone area. Local elevation reclassification was applied to dense stands of reeds, based on the assumption that reed height was relatively uniform. A systematic elevation subtraction was defined for these areas by measuring the mean elevation difference between reed stands and adjacent non-reed areas. Ninety-seven percent of the elevation errors that remained after these filters were applied were still in the range of ± 1 m. The sum of all TLS acquisition errors amounted to 0.07 m at most, so it was possible to attribute the large residual error to the presence of dense ground vegetation. This vegetation-derived error was removed using the GPS data. An error-thickness model was generated from the GPS/TLS difference values noted at 18 m intervals across the TLS coverage. This error-thickness model was then subtracted from the 1×1 m^2 TLS data to generate a TLS DSM.

It was not possible to externally validate the error that remained in the TLS DSM after the application of the error-thickness model correction, because no independent GPS points existed after DSM generation. Final cumulative elevation error in the TLS data was estimated by summing GPS measurement error, and cross-validation error from the interpolation of the error-thickness model. This suggested that 95% of the final elevation errors in the TLS DSM were within the range of ± 0.275 m. However, it should be noted that the errors returned from Leave One Out Cross Validation (LOOCV) probably overestimated final interpolation error (due to the reduction of local point sampling resolution during cross-validation). Therefore, the ± 0.275 m error range was probably conservative. Critically, these errors were small enough for the data to be used to externally validate elevation error in the photogrammetric DEM.

3.3. Optimised interpolation of photogrammetric DEM

The interpolation of the *x,y,z* medium-resolution DEM data was optimised in order to minimise the contribution of interpolation error to the overall error highlighted by external validation. Optimisation involved identification of global trends in the data, fitting the residual elevation values onto a suitable semi-variogram model, cross-validation of the kriging prediction, and generation of the final optimised kriging prediction (interpolation). Three overlapping elevation trends were isolated in the medium-resolution DEM, coinciding with; a north–south slope from land to sea (Fig. 4A); an east–west concavity of the coastline (Fig. 4B); and small hills on the east and west sides of the TLS survey area (Fig. 4C). A cumulative first/second/third order trend spherical semi-variogram model achieved the smallest variance between photogrammetric DEM point-pairs. This suggested that it took adequate account of global trends in the photogrammetric DEM and that it provided a good generalised model of spatial dependence in the elevation residuals (first (Fig. 5A), second (Fig. 5B) and third order (Fig. 5C) global trend removals).

Interpolation accuracy was verified using 50/50 and 67/33 training/test cross-validations and LOOCV. LOOCV involved the smallest hold-out, so it highlighted the smallest cross-validation errors. Three slightly different LOOCVs were applied to slightly different parameterisations of the Universal kriging prediction based upon the best performing semi-variogram model. All three

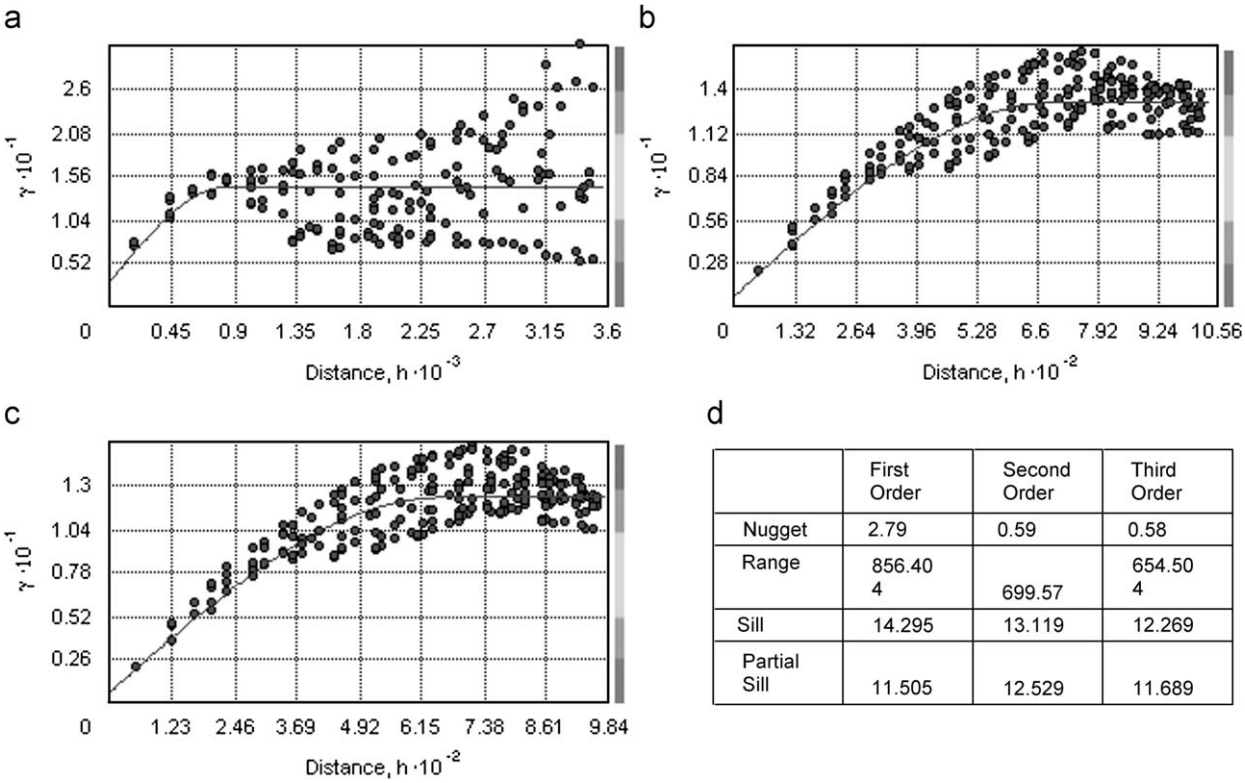

	First Order	Second Order	Third Order
Nugget	2.79	0.59	0.58
Range	856.404	699.57	654.504
Sill	14.295	13.119	12.269
Partial Sill	11.505	12.529	11.689

Fig. 5. . Global semi-variogram models for interpolation of photogrammetric DEM based on consideration of (A) first order trend, (B) first and second order trends, and (C) first, second and third order trends. (Dotted lines on each of the semi-variograms correspond with model error highlighted by the nugget effect). Note that points on scatter plots correspond with mean variances of all point-pairs within distance-defined bins rather than actual individual point-pairs.

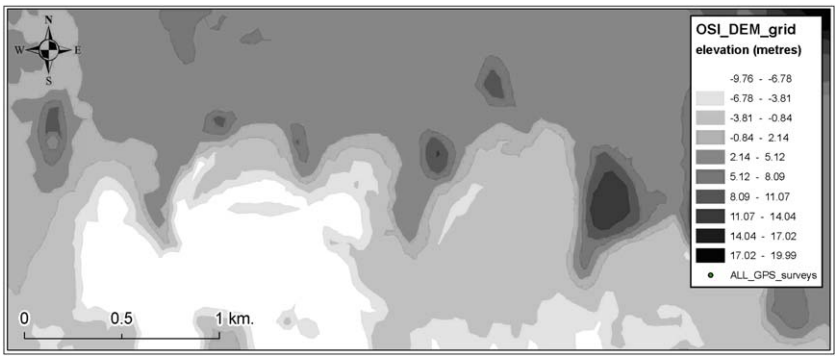

Fig. 6. . Universal kriging interpolation of photogrammetric DEM *x,y,z* point data.

produced almost identical results. The mean elevation error highlighted was 0.001 m and the standard deviation of the elevation errors was 0.25 m. Quoted error in the medium-resolution DEM was ± 3 m, so it was possible to conclude that any elevation errors detected by external-validation of the medium-resolution DEM would be justifiably attributable to DEM data error as opposed to errors introduced by interpolation.

3.4. External validation of medium-resolution DEM

External-validation was carried out using ArcGIS/ArcInfo (v9.2) Geostatistical Analyst. The optimised semi-variogram selected for interpolation of the photogrammetric DEM (Fig. 6) was used for the external-validation tests.

3.4.1. Validation using GPS

The post-processed and RTK-GPS points were combined into a single set (of 670 points at a mean sampling resolution of 40 m) and these data were used to externally validate the 100 ha test-section of the medium-resolution DEM. Just over 90% of all the medium-resolution DEM errors occurred within ± 3 m of zero, 96% of the errors occurred within ± 4 m, and 99% of the errors were within ± 6.5 m of zero (Table 5). Elevation errors within 10, 20, 40, 100 m of the coastline, and across the entire dataset were also assessed. A slight tendency for errors to increase with proximity to the coast was noted (Table 6). Therefore, the theory that elevation errors in the photogrammetric DEM might possibly have been smaller in the flatter portions of the study area could not be justified. The magnitude of the errors observed, and the spatial distribution of these errors suggested that the medium-resolution DEM was unsuitable for the spatial modelling of coastal inundation vulnerability in this location. However, the area was bisected with a reclamation barrier (Fig. 3) and drainage ditch that was relatively poorly represented by the spatial-resolution of the GPS validation points, so the results might have been biased by the spatial-resolution and scale at which the GPS data were acquired. The TLS DSM data point observations were used as an additional external validation set to determine what error might be highlighted using this higher-resolution larger-scale validation dataset.

3.4.2. Validation using TLS DSM

The TLS DSM *x,y,z* data provided 73,000 validation points across a 9 ha sub-section of the study area (Fig. 2c). The medium-resolution DEM was interpolated using the same procedure used for the GPS validation. Significantly larger elevation errors were highlighted relative to the results achieved using the lower-resolution GPS data. Ninety percent of the elevation errors identified were within the range of ± 4.25 m (Table 7), 95% of the errors occured in the ± 7 m range, and 99% of the errors were within in the range of ± 10 m. Similar to the trend observed when validated using GPS, medium-resolution DEM errors were larger (Table 8) near the coastline. These results confirmed that the elevation errors in the medium-resolution DEM were too large for the data to be used for the spatial prediction of coastal inundation risk. Errors of this magnitude would have compounded with the shallow gradient noted in the survey area (approximately 1:25) to result in horizontal misclassifications of inundation risk of the order of ± 175 m.

Table 5
Summary statistics for the elevation errors detected in the OSI DEM using the 670-point GPS external-validation dataset.

Count	670-point observations	
Mean error	-0.61m	
Std. Dev.	1.80m	
± 1 Std. Dev.	76%	490 points
± 2 m	77%	522 points
± 3 m	91%	616 points
± 4 m	96%	648 points
± 6.5 m	99%	669 points

Table 6
Measured elevation errors located within: 10, 20, 40 & 100 m from the coast, and across the entire GPS survey area.

Distance band (m)	Point count	Mean error (m)	Std. Dev. of errors (m)
10 m	101	−1.33	1.04
20 m	182	−1.13	1.33
40 m	292	−1.03	1.64
100 m	543	−0.69	1.66
Whole study area	675	−0.61	1.79

Table 7
Frequency distribution and summary statistics of elevation errors in the photogrammetric DEM identified by external-validation using the post-filtered T-LIDAR data.

Count	72,747
Mean error	−1.66m
Std. Dev.	2.30m
± 1 Std. Dev.	69%
± 4.25 m	90%
± 7 m	95%

Table 8
Measured elevation errors in the photogrammetric DEM located within 10, 20, 40, 60, 80, and 100 metres from the coast, and across the entire T-LIDAR validation dataset.

Distance band (m)	Point count	Mean error (m)	Std. Dev. of errors (m)
10 m	10,665	−2.09	1.06
20 m	19,984	−2.10	1.58
40 m	38,322	−2.32	2.31
60 m	53,912	−2.15	2.41
80 m	63,804	−1.91	2.31
100 m	69,330	−1.77	2.29
Whole study area	72,747	−1.66	2.30

Table 9
Elevation values for GPS points and T-LIDAR points located within 1, 2, 5 & 10 m of the highest available vector definition of mean high water (MHW) for Ireland.

Data	Statistic	1 m from MHW	2 m from MHW	5 m from MHW	10 m from MHW
GPS	Count	3	5	11	21
GPS	Min	1.41	1.09	1.09	1.09
GPS	Max	1.68	1.68	1.87	2.56
GPS	Mean	1.51	1.35	1.51	1.75
TLS	Count	457	921	2163	3490
TLS	Min	1.38	1.35	1.35	1.21
TLS	Max	2.4	2.41	2.68	3.07
TLS	Mean	1.63	1.63	1.65	1.74

4. Discussion

4.1. Suitability of the validation datasets used

Assessment of the elevation accuracies that were achieved with GPS and TLS confirmed their suitability for the external validation of elevation error. Vegetation-derived elevation errors in the TLS data were initially too large for the data to be used for validation, but it was possible to account for these errors using the GPS data as an alternative to last returns data during DSM generation.

4.2. Observed elevation error in the national photogrammetric DEM

Both the GPS and the TLS DSM validations revealed photogrammetric DEM elevation errors that were larger than the ± 3 m elevation error range quoted by the data suppliers. Ninety-five percent of the errors noted with 670 GPS points were in the range of ± 4 m, and 95% of the errors highlighted with 73,000 TLS DSM points were in the range of ± 7 m. The differential between the magnitude of the errors observed using each method appears to have been related to the higher density of the TLS points. The TLS data effectively represented the 2 m reclamation barrier and drainage ditch that bordered the study area, while the spatial-resolution of the GPS failed to do so.

The magnitude of the DEM error observed using both validation sets, and the tendency for these errors to increase with proximity to the coastline confirmed its unsuitability for the local spatial modelling of coastal inundation risk in the area where the study was carried out. The errors observed did not necessarily suggest that the quoted ± 3 m error statistic was inaccurate everywhere within the entire national coverage DEM. However, the magnitude of the error observed suggested that it would be unwise to use the medium-resolution DEM data for the spatial modelling of coastal inundation risk anywhere around the Irish coastline. Similar error ranges are often quoted for medium-resolution photogrammetric DEMs generated in locations other than Ireland (Lane et al., 2003; Lee et al., 2005; Oksanen and Sarjakoski 2005). While the results of our local assessment cannot be considered valid outside the limits of the area studied, the magnitude of the errors observed were sufficiently large relative to quoted DEM error to suggest caution when using similar data in any coastal context. Given the fact that even relatively modest elevation errors can result in significant horizontal misclassification of inundation risk on shallow gradient coastlines, it seems likely that photogrammetric DEM data may be susceptible to the same shortcomings elsewhere also. The fact that the DEM tested was provided at a spatial-resolution of 10 m also highlighted the risk of assuming that spatial resolution constitutes a reliable indicator of DEM accuracy. The 95% error range highlighted with TLS (± 7 m) was actually larger than the horizontal separation between the medium-resolution DEM points. This seems most likely to have arisen from the interpolation of the 10 metre DEM from much lower-resolution data. Based upon the available information (OSi, 2007) it seems that the medium-resolution DEM was generated from a combination of ground control and photogrammetric data at a substantially lower resolution. The 10 m DEM was derived from interpolation of 6 points per pair of overlapping stereo pairs (OSi, 2007). Assuming a standard 60% overlap on 1500×1000 m^2 aerial imagery, the mean resolution of 6 points on the 900×600 m^2 overlap between aerial stereo pairs would have been 300 m.

The segregation of DEM error source was not a primary concern of this study, but three main sources of error were apparent. These included: interpolation error, photogrammetric measurement error and the failure of a datum error. Interpolation error must have been a significant contributor to the overall error observed. Considering the fact the interpolation of the 10 metre points resulted in cross-validation errors of approximately 0.5 m, the interpolation of points at a mean sampling resolution of 300 m must have introduced even larger errors. The contribution of photogrammetric measurement error could not be segregated out from the total error observed, but some ground control points were used, so it seems likely that interpolation error was largest, and that photogrammetric measurement may not have been quite as large. It was possible to estimate datum error (deviation between map datum and local geoid). This revealed error of the order of 1.6 m (Table 9). The reliance on a limited number of ground control points, and the introduction of interpolation errors from low-resolution ground data can be expected to cause accuracy problems in any photogrammetric DEM. Datum error can be corrected for if suitable transformations are available, but the use of a limited number of ground points will always create difficulties.

4.3. Variation in elevation errors observed by each validation dataset

The differential noted between the magnitude of the errors highlighted by TLS and GPS appears to have been related to two main causes. Firstly, the TLS survey coincided (purely by chance) with the area where the largest errors were found in the GPS survey data (Table 6). Secondly, the GPS sample points were biased to a certain extent by survey point selection (by the principal author) towards accessible areas that were perceived to constitute a good 'average' representation of the elevation in the vicinity of each GPS sample point. This approach failed to take adequate account of high-frequency elevation anomalies (chiefly coinciding with a 2 m bank and 2 m ditch) that bisected the entire survey area. The spatial resolution of the TLS points enabled this bank and ditch feature to be represented at a much higher level of detail than GPS, thereby resulting in the identification of larger

elevation errors. The relatively close similarity of the 90% error highlighted by the GPS (± 3 m) and TLS (± 4.25) validations, supported the theory that the wide variation noted between the 95% error highlighted by GPS (± 4 m) and TLS (± 7 m) was related to the presence of the bank and ditch (which occupied roughly 5% of the survey area).

5. Conclusions

The principal aim of this paper was to accurately quantify elevation error in a coastal section of a medium-resolution DEM in a manner that clarifies the shortcomings of these types of DEMs for use in the spatial prediction of coastal inundation risk. Broad coverage medium-resolution and narrower coverage high-resolution validation datasets each highlighted significant elevation errors in the DEM tested, demonstrating how quoted global DEM error statistics can underestimate local elevation error. The observed tendency for these errors to increase with proximity to the coastline also demonstrated how a single global statistic for DEM can fail to account for local variations that may be important for the meaningful spatial prediction of local inundation risk.

While it was not intended to isolate the component contributors to the total error observed, DEM interpolation error, photogrammetric measurement error, and datum error appear to have constituted major sources of error. Errors arising from the interpolation and photogrammetric processing of a limited number of ground elevation measurements will tend to introduce problematic error into any photogrammetric DEM. Consideration of this issue may help to clarify the risks that are associated with using medium-resolution photogrammetric DEM data for the spatial prediction of coastal inundation risk.

The use of the TLS DSM data for validation highlighted a number of important issues. The TLS DSM data undoubtedly provided a very large number of validation points, and the acquisition accuracy of the data was very high. However, the magnitude of the vegetation-derived elevation error in the data prior to DSM processing was very large. TLS data were used in this paper in the absence of ALS data, and it is not suggested that TLS be used in preference to ALS data. However, the use of TLS in association with the GPS data did provide an accurate high-resolution validation dataset. It is important to note that ground vegetation would have been a problem if ALS data had been available for the study area also. Vegetation-derived errors of up to 1 m have been noted in studies that have used ALS DSM data to model environmental processes in coastal saltmarsh areas (Rosso et al., 2006), river floodplain areas (Cobby et al., 2001) and scrubland areas (Palamara et al., 2007). DEM and DSM users are generally not aware of this problem, so the quantification of the limitations of TLS and ALS in densely vegetated areas appears to offer potential for fruitful future research.

Acknowledgement

Research presented in this paper was funded by a Strategic Research Cluster grant (07/SRC/I1168) by Science Foundation Ireland under the National Development Plan. The authors gratefully acknowledge this support.

References

American National Standards Institute International Committee for Information Technology Standards (ANSI-INCITS), 1998. Information Technology – Spatial data transfer standard 320, http://mcmcweb.er.usgs.gov/sdts/standard.html, [accessed 7 January 2010].

Baldi, P., Bonvalot, S., Briole, P., Coltelli, M., Gwinner, K., Marsella, M., Puglisi, G., Rémy, D., 2002. Validation and comparison of different techniques for the derivation of digital elevation models and volcanic monitoring (Vulcano Island, Italy). International Journal of Remote Sensing 23, 4783–4800.

Bolstad, P.V., Stowe, T., 1994. An evaluation of DEM accuracy: elevation, slope, and aspect. Photogrammetric Engineering and Remote Sensing 60, 1327–1332.

Brasington, J., Rumsby, B.T., McVey, R.A., 2000. Monitoring and modelling morphological change in a braided Gravel-Bed River using high-resolution GPS-based survey. Earth Surface Processes and Landforms 25, 973–990.

Bryan, B., Harvey, N., Belperio, T., Bourman, B., 2001. Distributed process modelling for regional assessment of coastal vulnerability to sea-level rise. Environmental Modelling and Assessment 6, 57–65.

Chang, H.C., Ge, L.L., Rizos, C., Milne, T., 2004. Validation of DEMs derived from RADAR interferometry, Airborne laser scanning and photogrammetry by using GPS-RTK. In: Proceedings of Institute of Electrical and Electronics Engineers (IEEE) International Geoscience and Remote Sensing Symposium (IGARSS) '04, Alaska, USA. pp. 2815–2818.

Cobby, D.M., Mason, D.C., Davenport, I.J., 2001. Image processing of airborne scanning laser altimetry data for improved river flood modelling. International Society for Photogrammetry and Remote Sensing (ISPRS) Journal of Photogrammetry and Remote Sensing 56, 121–138.

Cowell, P.J., Zeng, T.Q., 2003. Integrating uncertainty theories with GIS for modeling coastal hazards of climate change. Marine Geodesy 26, 5–18.

Devoy, R.J.N., 2008. Coastal vulnerability and the implications of sea-level rise for Ireland. Journal of Coastal Research 24 (2), 325–341.

Dobosiewicz, J., 2001. Applications of digital elevation models and geographic information systems to coastal flood studies along the shoreline of Raritan bay New Jersey. Environmental Geosciences 8, 11–20.

Douglas, B.C., Kearney, M.S., Leatherman, S.P., 2001. Sea Level Rise: History and Consequences. Academic Press, California 232pp.

Ehlschlaeger, C.R., 2002. Representing multiple spatial statistics in generalized elevation uncertainty models: moving beyond the variogram. International Journal of Geographical Information Science 16, 259–285.

FGDC, 1998. Geospatial positioning accuracy standards, Part 3: National standard for spatial data accuracy, Federal Geographic Data Committee, FGDC-STD-007.3-1998, USA, 25 pp.

Fisher, P., 1998. Improved modelling of elevation error with geostatistics. GeoInformatica 2, 215-233.

Fisher, P.F., Tate, N.J., 2006. Causes and consequences of error in digital elevation models. Progress in Physical Geography 30 (4), 467–489.

Flood, M., 2004. American Society for Photogrammetry and Remote Sensing (ASPRS) Guidelines – Vertical accuracy reporting for LiDAR data, version 1.0, ASPRS LiDAR Committee (PAD), 20pp. http://www.asprs.org/society/committees/lidar/Downloads/Vertical_Accuracy_Reporting_for_Lidar_Data.pdf.

Gao, Y., Chen, K., 2004. Performance analysis of precise point positioning using real-time orbit and clock products. Journal of Global Positioning Systems 3 (1-2), 95–100.

Gomes Pereira, L.M., Wicherson, R.J., 1999. Suitability of laser data for deriving geographical information: a case study in the context of management of fluvial zones. International Society for Photogrammetry and Remote Sensing (ISPRS) Journal of Photogrammetry & Remote Sensing 54, 105–114.

Gornitz, V., Couch, S., Hartig, E.K., 2002. Impacts of sea level rise in the New York City metropolitan area. Global and Planetary Changes 32, 61–88.

Hall, S.A., Burke, I.C., Box, D.O., Kaufmann, M.R., Stoker, J.M., 2005. Estimating stand structure using discrete-return lidar: an example from low density, fire prone ponderosa pine forests. Forest Ecology and Management 208, 189–209.

Heuvelink, G.B.M., 1998. Error Propagation in Environmental Modelling with GIS. Taylor & Francis, London 150pp.

Hodgson, M.E., Bresnahan, P., 2004. Accuracy of airborne LiDAR-Derived elevation: empirical assessment and error budget. Photogrammetric Engineering and Remote Sensing 70 (3), 331–339.

Hodgson, M.E., Jensen, J.R., Schmidt, L., Schill, S., Davis, B., 2003. An evaluation of LIDAR- and IFSAR-derived digital elevation models in leaf-on conditions with USGS Level 1 and Level 2 DEMs. Remote Sensing of Environment 84, 295–308.

Höhle, J., Potuckova, M., 2006. The EuroSDR Test: Checking and Improving of Digital Terrain Models, in Eurosdr European Spatial Data Research. Official publication No. 51, EuroSDR publications, Frankfurt, Germany 188pp.

Holmes, K.W., Chadwick, O.A., Kyriakidis, P.C., 2000. Error in a USGS 30-meter digital elevation model and its impact on terrain modelling. Journal of Hydrology 233, 154–173.

Hughes, R.G., Paramor, O.A.L., 2004. On the loss of saltmarshes in south-east England and methods for their restoration. Journal of Applied Ecology 41, 440–448.

Huising, E.J., Gomes Pereira, L.M., 1998. Errors and accuracy estimates of laser data acquired by various laser scanning systems for topographic applications. International Society for Photogrammetry and Remote Sensing (ISPRS) Journal of Photogrammetry and Remote Sensing 53, 245–261.

Iavaronea, A., Vagners, D., 2003. Sensor fusion: generating 3D by combining airborne and tripod-mounted LIDAR data. In: Proceedings of the International Workshop on Visualization and Animation of Reality-Based 3D Models 2003, Engadin, Switzerland, International Archives of the Photogrammetry, Remote Sensing and Spatial Information Sciences 34, W10.

Intergovernmental Panel on Climate Change (IPCC), 2007. Summary for policymakers. In: Solomon, S., Qin, D., Manning, M., Chen, Z., Marquis, M., Averyt, K.B., Tignor, M., Miller, H.L. (Eds.), Climate Change 2007: The Physical Science Basis.. Cambridge University Press, Cambridge, United Kingdom and New York, NY, USA 21pp.

Lane, S.N., Westaway, R.M., Murray-Hicks, D., 2003. Estimation of erosion and deposition volumes in a large gravel-bed braided river using synoptic remote sensing. Earth Surface Processes and Landforms 28, 249–271.

Leatherman, S.P., Douglas, B.C., Labrecque, J.L., 2003. Sea level and coastal erosion require large-scale monitoring. Transactions American Geophysical Union (EOS) 84 (2 doi:, doi:10.1029/2003EO020001.

Lee, I., Chang, H.C., Ge, L.L., 2005. GPS campaigns for validation of InSAR derived DEMs. Journal of Global Positioning Systems 4, 82–87.

Leica Geosystems, 2007. High Definition Surveying: Training Manual, Leica Geosystems, Munich, Germany, p.176.

Lim, K., Treitz, P., Wulder, M., St-Onge, B., Flood, M., 2003. LiDAR remote sensing of forest structure. Progress in Physical Geography 27, 88–106.

Lohani, B., Mason, D.C., 2001. Application of airborne scanning laser altimetry to the study of tidal channel geomorphology. International Society for Photogrammetry and Remote Sensing (ISPRS) Journal of Photogrammetry and Remote Sensing 56, 100–120.

McInnes, K.L., Walsh, K.J.E., Hubbert, G.D., Beer, T., 2003. Impact of sea-level rise and storm surges on a coastal community. Natural Hazards 30, 187–207.

Oksanen, J., Sarjakoski, T., 2005. Error propagation analysis of DEM-based drainage basin delineation. International Journal of Remote Sensing 26, 3085–3102.

Orford, J., 1989. A review of tides currents and waves in the Irish Sea. In: Sweeney, J. (Ed.), The Irish Sea: A Resource at Risk. Special Publication No. 3. Geographical Society of Ireland, Dublin, Ireland, pp. 18–46.

Palamara, D.R., Nicholson, M., Flentje, P., Baafi, E., Brassington, G.M., 2007. An evaluation of airborne laser scan data for coalmine subsidence mapping. International Journal of Remote Sensing 28, 3181–3203.

Popescu, S.C., Wynne, R.H., Nelson, R.F., 2002. Estimating plot-level tree heights with lidar: local filtering with a canopy-height based variable window size. Computers and Electronics in Agriculture 37, 71–95.

Pugh, D.T., 2004. Changing sea levels: effects of tides, Weather and Climate. Cambridge University Press, Cambridge 255pp.

Rosso, P.H., Ustin, S.L., Hastings, A., 2006. Use of LiDAR to study changes associated with Spartina invasion in San Francisco bay marshes. Remote Sensing of Environment 100, 295–306.

Ruiz, A., Kornus, W., Talaya, J., Colomer, J.L., 2004. Terrain modelling on an extremely steep mountain: a combination of airborne and terrestrial LiDAR. In: Proceedings of 20th International Society for Photogrammetry and Remote Sensing (ISPRS) Congress on Geo-imagery Bridging Continents, Istanbul, Turkey, pp. 1–4.

Sithole, G., Vosselman, G., 2004. Experimental comparison of filter algorithms for bare-earth extraction from airborne laser scanning point clouds. International Society for Photogrammetry and Remote Sensing (ISPRS) Journal of Photogrammetry and Remote Sensing 59, 85–101.

United States Geological Survey (USGS), 2006. Land-based LiDAR mapping – a new surveying technique to shed light on rapid topographic change. USGS Fact Sheet No. 3111, USGS, 4pp.

Van Niel, K.P., Austin, M.P., 2007. Predictive vegetation modelling for conservation: impact of error propagation from digital elevation data. Ecological Applications 17, 266–280.

Van Niel, K.P., Laffan, S.W., Lees, B.G., 2004. Effect of error in the DEM on environmental variables for predictive vegetation modelling. Journal of Vegetation Science 15, 747–756.

Webster, T.L., 2005. LIDAR validation using GIS: a case study comparison between town LIDAR collection methods. Geocarto International 20, 11–19.

Wechsler, S.P., Kroll, C.N., 2006. Quantifying DEM uncertainty and its effect on topographic parameters. Photogrammetric Engineering and Remote Sensing 72, 1081–1090.

Wolters, M., Bakker, J.P., Bertness, M.D., Jefferies, R.L., Möller, I., 2005. Saltmarsh erosion and restoration in south-east England: squeezing the evidence requires realignment. Journal of Applied Ecology 42, 844–851.